DOI: 10.1002/chem.200501082

trans–cis Photoisomerization of the Styrylpyridine Ligand in $[Re(CO)_3(2,2'\text{-bipyridine})(t\text{-4-styrylpyridine})]^+$: Role of the Metal-to-Ligand Charge-Transfer Excited States

Julien Bossert and Chantal Daniel*[a]

Abstract: The *trans-cis* isomerization of the styrylpyridine carbon–carbon double bond induced by visible light irradiation in *fac*-$[Re(CO)_3(bpy)(stpy)]^+$ (bpy = 2,2′-bipyridine; stpy = *t*-4-styrylpyridine) has been investigated by means of quantum-chemical methods. The structures of the various *cis* and *trans* conformers of $[Re(CO)_3(bpy)(stpy)]^+$ have been optimized at the density functional theory (DFT) level. Three rotational conformers for the most stable *trans* isomer lie within 2.3 kJ mol^{-1} each other. The energy difference between the *cis* and *trans* isomers is 27.0 kJ mol^{-1}. The electronic spectroscopy of the most stable conformers has been investigated by time-dependent DFT (TD-DFT) and complete active space self-consistent field/CAS second order perturbation theory (CASSCF/CASPT2) calculations. The lowest absorption bands are dominated by metal-to-ligand charge-transfer (MLCT, $d_{Re}\rightarrow\pi^*_{bpy}$) transitions calculated at about 25000 cm^{-1} and by a strong intraligand ^{1}IL ($\pi_{stpy}\rightarrow\pi^*_{stpy}$) transition in the near UV region. On the basis of CASSCF potential energy curves (PECs) calculated as a function of the torsion angle of the C=C bond of the styrylpyridine ligand, it is shown that the role of the low-lying MLCT states is important in the photoisomerization mechanism. In contrast to the free organic ligand, in which the singlet mechanism is operational via the ^{1}IL (S_1) and electronic ground (S_0) states, coordination to the rhenium steers the isomerization to the triplet PEC corresponding to the ^{3}IL state. From the ^3IL_t (t = *trans*) the system evolves to the perpendicular intermediate ^3IL_p (p = perpendicular) following a 90° rotation around the styrylpyridine C=C bond. The metal center acts as a photosensitizer because of the presence of photoactive MLCT states under visible irradiation. The position of the crossing between the ^{3}IL and electronic ground state PEC determines the quantum yield of the isomerization process.

Keywords: charge transfer · density functional calculations · photoisomerization · rhenium

Introduction

Third-row transition-metal complexes substituted by acceptor ligands are widely studied for their fascinating photophysical properties. After irradiation under visible light several routes are opened towards various processes, such as electron/energy transfer, luminescence, ultrafast dissociation, and isomerization.[1,2] Photochromic molecules and their photoisomerization reactions have been the subject of a number of experimental studies.[3,4] A series of rhenium(I) diimine complexes with photoisomerizable pyridyl-azo, -ethenyl, or -ethyl ligands have been investigated for their photochemical, electrochemical, and photophysical properties.[5] The *trans*→*cis* photoisomerization of $[Re(CO)_3(bpy)(stpy)]^+$ was observed for the first time in the course of these experiments. The photoizomerisation quantum yield determined for similar complexes with a NO_2-substituted styrylpyridine ligand ranges between 0.47 and 0.66.[5] The ultrafast excited-state dynamics of *fac*-$[Re(Cl)(CO)_3(t\text{-4-styrylpyridine})_2]$ and *fac*-$[Re(t\text{-4-styrylpyridine})(CO)_3(2,2'\text{-bipyridine})]^+$ have been investigated in recent picosecond/femtosecond time-resolved spectroscopy experiments (Resonance Raman, emission, absorption) in the condensed phase.[6] It has been shown that the *trans–cis* isomerization mechanism is characterized by a switch from a spin singlet to a triplet ππ* excited state's potential energy surface. The rhenium(I) center acts as an intramolecular triplet sensitizer, facilitating the $^1\pi\pi^*\rightarrow{}^3\pi\pi^*$ intersystem crossing within the femtosecond range. An indirect population of the reactive ^{3}IL (ππ*) state by a picosecond ^{3}MLCT ($d_{Re}\rightarrow\pi^*_{bpy}$) internal conversion is proposed in the case of fac-$[Re(stpy)(CO)_3(bpy)]^+$.

[a] J. Bossert, Dr. C. Daniel
Laboratoire de Chimie Quantique
UMR 7551 CNRS/Université Louis Pasteur
4 Rue Blaise Pascal, 67000 Strasbourg (France)
E-mail: daniel@quantix.u-strasbg.fr

Whereas the *trans–cis* photoisomerization of an olefinic C=C bond is well documented for organic stilbene-like molecules, both in terms of experimental and theoretical studies,[7–9] the mechanism governing this process in ligands coordinated to transition metals is not known.

The aim of the present work based on accurate quantum-chemical calculations is twofold: 1) the theoretical description of the *trans*→*cis* photoisomerization mechanism of the title molecule and 2) comparison with the photoisomerization mechanism that occurs under UV irradiation in organic molecules.

Computational Methods

The geometric structures of the conformers of each *trans* and *cis* isomer of $[Re(stpy)(CO)_3(bpy)]^+$ have been optimized by means of density functional theory (DFT)[10] with no symmetry constraints with the B3LYP functional.[11]

The electronic configuration of $[Re(stpy)(CO)_3(bpy)]^+$ in its ^1A ground state is given by $(5d_{yz})^2(5d_{xz})^2(5d_{xy})^2$ with 284 electrons. The electronic structure of the ground and excited states of the lowest conformers of each *trans* and *cis* isomer were calculated at the complete active space self-consistent field/multi state-CAS perturbation theory second order (CASSCF/MS-CASPT2) level of theory[12,13] and by means of time-dependent DFT calculations.[14] Eight electrons (the six 5d electrons and the two π_{stpy} electrons) were correlated into nine active orbitals: the four doubly occupied orbitals in the electronic ground state, the 5d′ orbitals of correlation, and the two lowest π^*_{bpy} and π^*_{stpy} vacant orbitals. The vacant 5d orbitals of the rhenium are too high in energy to play a role in the spectroscopy and do not contribute to the active space represented in Figure 1.

The level-shift technique was applied to the MS-CASPT2 calculations to avoid intruder-state problems and the stability of the perturbative treatment was tested with values in the 0.0–0.4 hartree range.[15]

To choose appropriate basis sets adapted to the correlated methods, the theoretical problem, and the size of the molecule, various basis sets were tested at the CASSCF/MS-CASPT2 level on the model system $[Re(CO)_3(bpy)(NHCH_2)]^+$.[16] For this model system eight electrons were correlated in fourteen active orbitals and the CASSCF was averaged over the ten lowest $^1A'$ states. MS-CASPT2 calculations were performed on the basis of this CASSCF wave function with a level shift of 0.2 hartree. The following basis sets were tested: the relativistic pseudopotentials of Stuttgart and associated valence basis sets[17] on all atoms (without and with polarized d functions on the second row atoms) and the pseudopotentials of Stuttgart with associated valence basis sets on the metal centre combined either with the Dunning double-ξ polarized (DZP) basis functions[18] or with the atomic natural orbitals small (ANO-S)[19] on the second-row atoms. A last test was performed with the Dunning's correlation consistent double-ξ polarized (cc-pVDZ) basis sets[20] on the second-row atoms. ANO-S and DZP basis sets on the second-row atoms combined with the ECP of Stuttgart on the rhenium atom gave nearly identical descriptions of the excited states of the model complex and mean deviations on MS-CASPT2 transition energies on the order of 150 cm^{-1}. The use of pseudopotentials on all atoms, even with polarized d functions on the second-row atoms, led to large qualitative and quantitative differences in the electronic spectroscopy assignment of $[Re(CO)_3(bpy)(NHCH_2)]^+$.[16]

For the geometric optimizations of the real complex $[Re(stpy)(CO)_3(bpy)]^+$, relativistic pseudopotentials of Stuttgart were used with the following valence basis sets: a (8 s7p6d) set contracted to [6s5p3d] for the rhenium atom (Z_{eff} = 15.0), a (4 s4p) set contracted to [2s2p] for the carbon (Z_{eff} = 4.0) and nitrogen (Z_{eff} = 5.0) atoms, and a (4 s5p) set contracted to [2s3p] for the oxygen atom (Z_{eff} = 6.0).

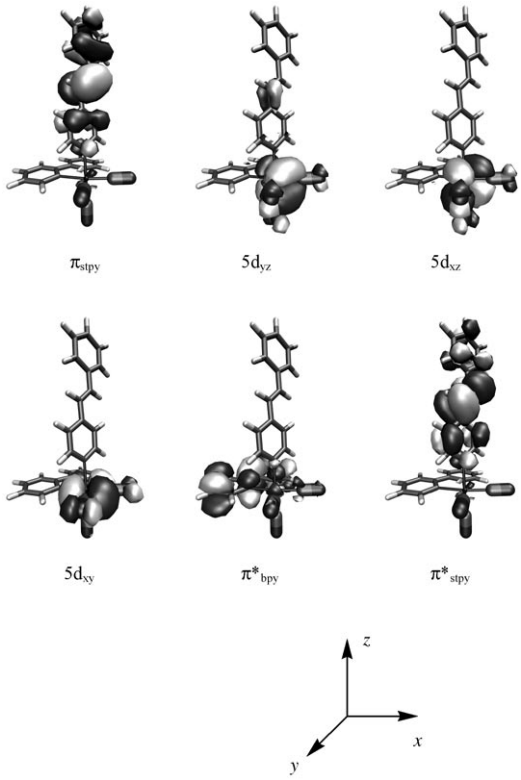

Figure 1. The six active orbitals most relevant for the electronic spectroscopy for the most symmetric isomer of *trans*-$[Re(stpy)(CO)_3(bpy)]^+$.

The excited state calculations of $[Re(stpy)(CO)_3(bpy)]^+$ were performed with the following basis sets for the second row atoms: the Dunning double-ξ polarized sets (9 s5p1d) contracted to [4s2p1d] at the TD-DFT level and the ANO-S sets (10 s6p3d) contracted to (3 s2p1d) at the CASSCF/MS-CASPT2 level.

The potential energy curves (PECs) corresponding to the low-lying singlet and triplet states correlating the *trans*-$[Re(stpy)(CO)_3(bpy)]^+$ isomer to the *cis*-$[Re(stpy)(CO)_3(bpy)]^+$ isomer were calculated as a function of the double-bond torsion angle, which is the driving coordinate of the isomerization process as shown for the stilbene, for instance in Figure 2.[7]

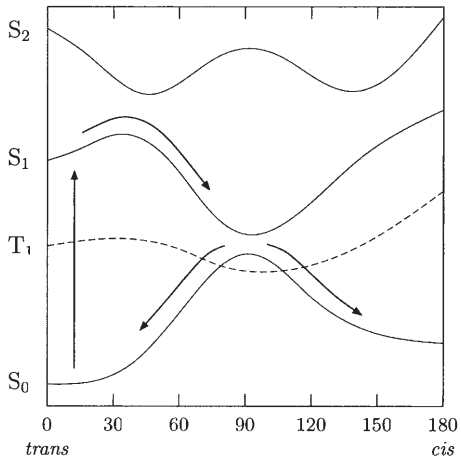

Figure 2. The PECs corresponding to the low-lying singlet and triplet states correlating the *trans*-$[Re(stpy)(CO)_3(bpy)]^+$ isomer to the *cis*-$[Re(stpy)(CO)_3(bpy)]^+$ isomer calculated as a function of the double-bond torsion angle, as shown for the stilbene.

According to the size of the molecular system, the low symmetry of the process, and the high density of electronic states in the UV/Vis domain of energy, other methods such as a systematic search for minimum energy paths or critical geometries from the Franck–Condon point are definitely impracticable. The present ab initio calculations are at the limit of what can currently be done on these large molecules. The TD-DFT calculations were performed with Gaussian 98[21] and the ab initio calculations with MOLCAS 5.0 Quantum Chemistry software.[22]

Results and Discussion

Structures of the various conformers of *trans*-[Re(stpy)(CO)$_3$(bpy)]$^+$ and *cis*-[Re(stpy)(CO)$_3$(bpy)]$^+$: The DFT-optimized geometries of the two isomers of [Re(stpy)(CO)$_3$(bpy)]$^+$ for the different conformers are represented in Figure 3 with the relative energies in kJ mol^{-1} and eV. The geometry optimizations produce three rotational conformers for the *trans* isomer within 2.3 kJ mol^{-1} (or 0.024 eV) and four rotational conformers for the *cis* isomer within 3.3 kJ mol^{-1} (0.034 eV). The energy difference between the two isomers is 27.0 kJ mol^{-1} (0.28 eV).

The rotamer with the most stable calculated structure corresponds to that established by means of NMR studies of similar complexes in solution.[23] Characteristic bond lengths and bond angles of [Re(stpy)(CO)$_3$(bpy)]$^+$ are given in Table 1 for the *trans* and *cis* isomers and are compared with the values for the X-ray structure of a photoisomerizable derivative of [Re(stpy)(CO)$_3$(bpy)]$^+$ represented in Figure 4.[24] The CASSCF-optimized bond lengths and bond angles of the *cis*-stilbene are also reported for comparison.

The *trans*-styrylpyridine is planar in the complex, like in the uncoordinated 2-*trans*-styrylpyridine or the 2,6-di-*trans*-styrylpyridine.[25] The central double bond is identical in both isomers (calcd: 1.358–1.359 Å). It can be compared with the X-ray data (1.320 Å)[26] or to the CASSCF-optimized value in the stilbene (1.352 Å).[27] When going from the *trans* to the *cis* isomer the distances between the aromatic groups and the ethylenic bond increase by 0.01 Å, which leads to a small decrease in the conjugation relative to the *trans* form. The bond length with the pyridinic cycle (C16–C19) is shorter than the one with the benzenic cycle (C20–C21), which is close to the typical value of 1.470 Å. The deformations of the *cis*-styrylpyridine are due to the steric interactions between the two rings. The main consequence is a destabilization of the *cis* isomers with respect to the *trans* isomers, owing to a decrease of the conjugation between the aromatic rings and the ethylenic bond.

Otherwise, the DFT-optimized structures of the two isomers are very similar and agree rather well with the experimental data available for the surfactant derivative of [Re(stpy)(CO)$_3$(bpy)]$^+$.

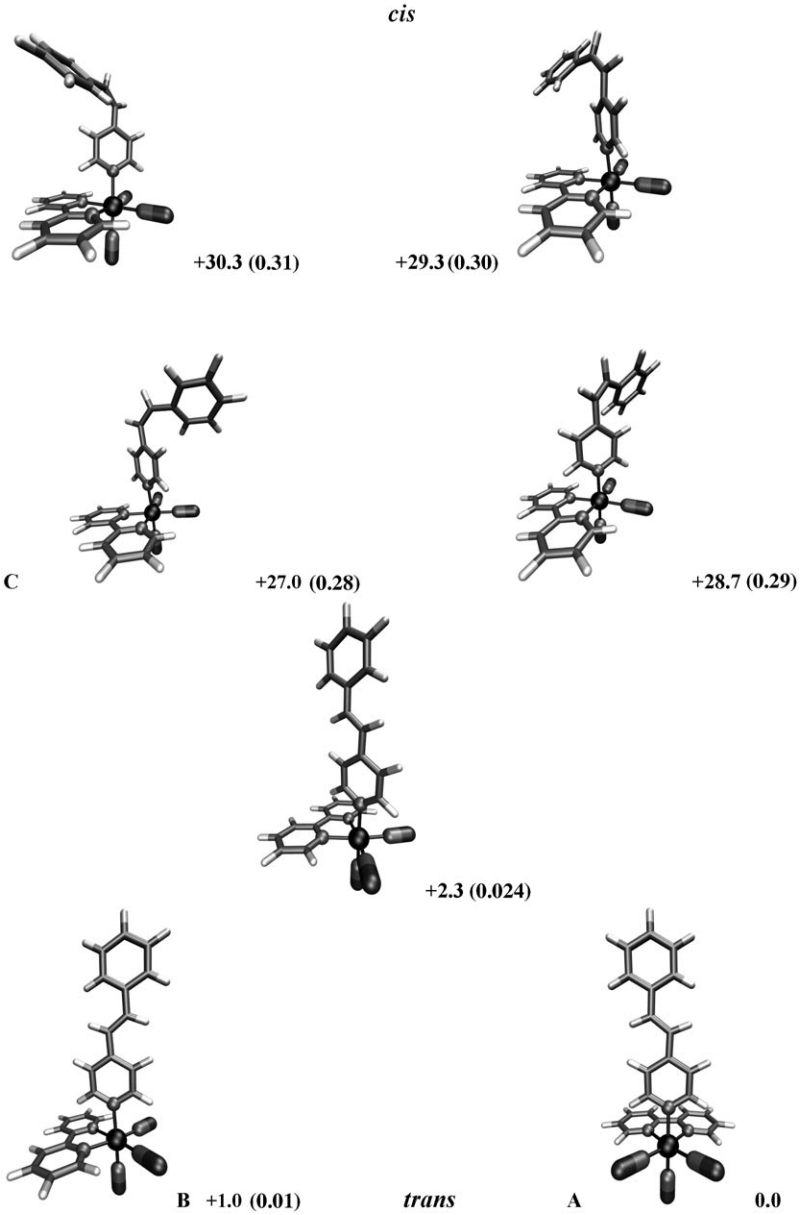

Figure 3. Optimized structures of the *cis*-and *trans*-[Re(CO)$_3$(bpy)(stpy)]$^+$ isomers. The relative energies are in kJ mol^{-1} (and eV) with respect to the most stable conformer A.

Table 1. Bond lengths [Å] and bond angles [°] of $[Re(CO)_3(bpy)(stpy)]^+$. The numbering of the atoms corresponds to Figure 4.

	trans	*cis*	X-ray[a]	*cis*-Stilbene[b]
Re–N1	2.202–2.205	2.202–2.206	2.177 (4)	
Re–N2	2.202–2.205	2.202–2.206	2.176 (6)	
Re–N3	2.245–2.249	2.246–2.251	2.219 (4)	
Re–C1	1.943–1.945	1.943–1.945	1.928 (7)	
Re–C2	1.951	1.951	1.927 (9)	
Re–C3	1.951	1.951	1.927 (9)	
N1-Re-N2	74.4–74.6	74.4–74.6	75.0 (2)	
N1-Re-C3	97.5–97.8	97.4–97.9	99.4 (2)	
N1-Re-C4	97.5–97.8	97.4–97.9	98.6 (2)	
C1-Re-C3	90.6–89.8	90.7–89.7	86.9 (3)	
C19–C20	1.358–1.359	1.358–1.359	1.320 (8)	1.352
C20–C21	1.459	1.471–1.472		1.488
C16–C19	1.453	1.464–1.465		1.488
C16-C19-C20	126	131		
C19-C20-C21	127	131–132		
C16-C19-C20-C21	9–10	9–10		
C17-C16-C19-C20	0	35–37		43.5
C19-C20-C21-C22	0	25–27		43.5

[a] From ref. [23]. [b] From ref. [26]

Qualitative analysis of the absorption spectra of *trans*-$[Re(stpy)(CO)_3(bpy)]^+$ and *cis*-$[Re(stpy)(CO)_3(bpy)]^+$ by TD-DFT: The UV/Vis absorption spectrum of $[Re(stpy)(CO)_3(bpy)]^+$ recorded in acetonitrile[6,28] exhibits one broad band between 400 and 300 nm centered at about 332 nm, which is assigned to a stpy-localized intraligand (^{1}IL) transition ($\pi_{stpy}\rightarrow\pi^*_{stpy}$), with a spike at 320 nm attributed to a bpy-localized IL transition (Figure 5).

The unusually high molar absorptivity of this band and resonance Raman spectra indicate that this IL band contains contributions from metal-to-ligand charge-transfer (MLCT) states. A weak tail extending to about 420 nm is attributed to an MLCT transition corresponding to a $d_{Re}\rightarrow\pi^*_{bpy}$ excitation. The upper part of the spectrum is not assigned.

The low-lying singlet and triplet states of $[Re(stpy)(CO)_3(bpy)]^+$ obtained by TD-DFT calculations are reported in Table 2 for the trans (conformers A and B, Figure 3) and *cis* (conformer C, Figure 3) isomers.

The electronic spectra of the *trans* and *cis* isomers are qualitatively similar and contain a series of low-lying ^{1,3}MLCT transitions corresponding to $d_{Re}\rightarrow\pi^*_{bpy}$ excitations (calcd between 20000 cm^{-1} and 25000 cm^{-1}; 400–500 nm). The two highest states are nearly degenerate at about 23500 cm^{-1} (425 nm) with significant oscillator strengths, the values of which depend on the conformer. The next absorbing states, which are very close in energy, correspond to ligand-to-ligand charge transfer (LLCT) ($\pi_{stpy}\rightarrow\pi^*_{bpy}$) and IL ($\pi_{stpy}\rightarrow\pi^*_{stpy}$) transitions calculated between 25880 and 26730 cm^{-1} (at about 385 nm), depending on the isomers with a strong oscillator strength for the IL state (nearly 1.0 in the *trans* isomer). This state is characterized by an excitation localized at the level of the C=C bond of the stpy ligand, seat of the

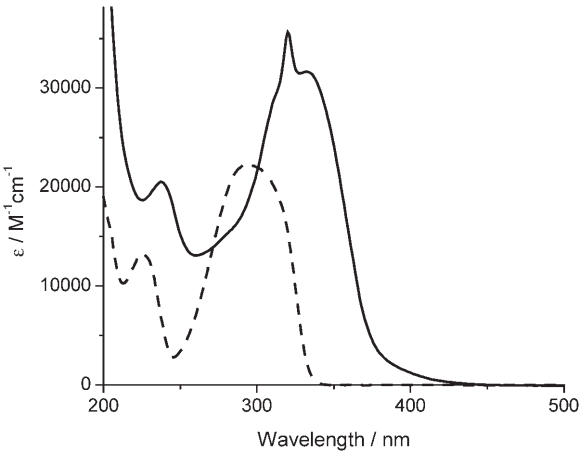

Figure 5. UV/Vis absorption spectrum of stpy (-----) and $[Re(CO)_3(bpy)(stpy)]^+$ (——) in acetonitrile.[27]

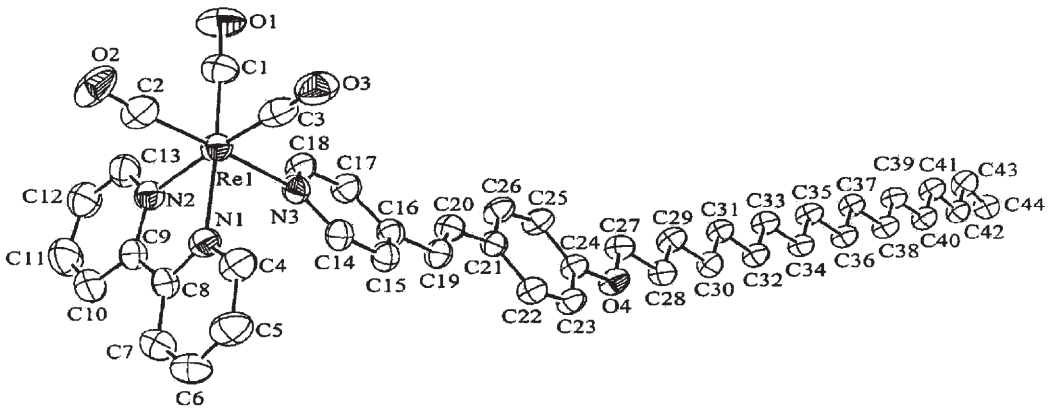

Figure 4. The $[Re(CO)_3(bpy)(stpy)]^+$ derivative for which the photoisomerization has been observed in the visible.[23]

Table 2. TD-DFT transition energies [cm^{-1}] of $[Re(CO)_3(bpy)(stpy)]^+$ and associated oscillator strengths.

States	*trans* conformer A	*trans* conformer B	*cis* conformer C
^{3}IL (stpy)	16470	16450	17940
^{3}LLCT (stpy→bpy)	18070	17610	18850
^{1}LLCT (stpy→bpy)	**18520** *0.0126*	**17900** *0.0008*	**19320** *0.0147*
^{3}MLCT (Re→bpy)	20240	21000	20350
^{3}MLCT (Re→bpy)	21680	21300	21750
^{1}MLCT (Re→bpy)	21690 *0.0025*	22020 *0.0019*	21830 *0.0024*
^{3}MLCT (Re→bpy)	22980	22970	23110
^{1}MLCT (Re→bpy)	23160 *0.0088*	23090 *0.0134*	23290 *0.0156*
^{1}MLCT (Re→bpy)	**23620** *0.0655*	**23850** *0.0989*	**23610** *0.0577*
^{3}IL (bpy)	24790	24590	24800
^{3}LLCT (stpy→bpy)	25180	25000	24870
^{1}LLCT (stpy→bpy)	25210 *0.0003*	25000 *0.0*	24880 *0.0*
^{1}LLCT (stpy→bpy)	26030 *0.1765*	25880 *0.0009*	27030 *0.0307*
^{1}IL (stpy)	**26730** *0.9663*	**26270** *1.1095*	**25740** *0.3779*

isomerization process. The corresponding ^{3}IL state, which may play an important role in the mechanism, is the lowest triplet state, with a transition energy of about 16500 cm^{-1}. A low-lying LLCT state is calculated at 18520 (*trans* isomer A) or 17940 cm^{-1} (*cis* isomer C) (at about 550 nm) with a significant oscillator strength. The TD-DFT transition energies are shifted to the red relative to the experimental bands (by 4000 cm^{-1} or 0.5 eV) for the ^{1}IL state localized on the stpy ligand. The theoretical spectrum disagrees with the proposed assignment through the presence of a low-lying LLCT state that is not observed in the experimental spectrum. The presence of this state in the lowest part of the theoretical spectrum could be an artefact of TD-DFT, which tends to underestimate the transition energies to the long-range CT[29–31] such as the one in this case which corresponds to a stpy to bpy excitation. Moreover there is no evidence from the calculations of an IL bpy-localized state which was anticipated at 320 nm. Rather good agreement is obtained for the MLCT states. To explore the electronic spectroscopy of $[Re(stpy)(CO)_3(bpy)]^+$ in more detail, CASSCF/MS-CASPT2 calculations were performed.

Theoretical analysis of the absorption spectrum of *trans*-$[Re(stpy)(CO)_3(bpy)]^+$ by CASSCF/MS-CASPT2 calculations: Ab initio calculations were performed on the most symmetric isomer of *trans*-$[Re(stpy)(CO)_3(bpy)]^+$, namely the conformer B (Figure 3). Eight electrons (six d_{Re} electrons and two π_{stpy} electrons) were correlated in nine active orbitals, the six active orbitals most relevant for the electronic spectroscopy are depicted in Figure 1. The choice of the CASSCF characteristics was based on the knowledge of the experimental spectrum and on the preliminary TD-DFT results. The CASSCF and MS-CASPT2 transition energies are reported in Table 3.

The CASSCF absorption spectrum is qualitatively similar to the TD-DFT spectrum with the ^{3}IL ($\pi_{stpy}\rightarrow\pi^*_{stpy}$) state as the lowest triplet state followed by a series of ^{1,3}MLCT states corresponding to $d_{Re}\rightarrow\pi^*_{bpy}$ excitations. The upper part of the spectrum is characterized by two nearly degenerate singlets, namely the ^{1}IL ($\pi_{stpy}\rightarrow\pi^*_{stpy}$) state and the ^{1}LLCT state corresponding to the $\pi_{stpy}\rightarrow\pi^*_{bpy}$ excitation. In contrast to the TD-DFT results and in agreement with the experimental data, the CASSCF spectrum does not indicate the presence of low-lying LLCT states. CASSCF calculations are only qualitative and lead to overestimated transition energies, by nearly 1.0 eV for the ^{1}IL ($\pi_{stpy}\rightarrow\pi^*_{stpy}$) and the ^{1}MLCT states. The large singlet–triplet energy gap of 12000 cm^{-1} found for the ^{1}IL state is characteristic of the transitions corresponding to $\pi_{stpy}\rightarrow\pi^*_{stpy}$ excitations in organic free ligands. The calculated oscillator strengths follow the experimental and TD-DFT trends and correctly reproduce the relative intensities of the ^{1}IL and ^{1}MLCT states. The ^{1}MLCT states are correctly described at the MS-CASPT2 level, the transition energies were calculated to be 23550 (425 nm), 25840 (387 nm), and 26800 cm^{-1} (373 nm), the two highest states having significant oscillator strengths. These MLCT states definitively contribute to the experimental band observed between 400 and 300 nm. The ^{3}IL ($\pi_{stpy}\rightarrow\pi^*_{stpy}$) state was calculated to be at 20990 cm^{-1} and remains the lowest triplet state at the MS-CASPT2 level.

Table 3. CASSCF and MS-CASPT2 transition energies [cm^{-1}], associated wavelengths [nm] and oscillator strengths [f] of *trans*-$[Re(CO)_3(bpy)(stpy)]^+$ conformer B of C_s symmetry (see Figure 3).

State	One-electron excitation in the main configuration	CASSCF[a]	λ	f	MS-CASPT2	λ
^{3}IL a^3A'	$\pi_{stpy}\rightarrow\pi^*_{stpy}$ (92%)	25550 (24530)			20990	
a^3MLCT b^3A'	$5d_{yz}\rightarrow\pi^*_{bpy}$ (81%)	26470 (25280)			24190	
b^3MLCT c^3A'	$5d_{x^2-y^2}\rightarrow\pi^*_{bpy}$ (81%)	28000 (25840)			25990	
c^3MLCT a^3A''	$5d_{xz}\rightarrow\pi^*_{bpy}$ (90%)	28790 (28060)			23170	
a^1MLCT a^1A''	$5d_{xz}\rightarrow\pi^*_{bpy}$ (91%)	29140 (29860)	343	0.011	23550	425
b^1MLCT b^1A'	$5d_{x^2-y^2}\rightarrow\pi^*_{bpy}$ (60%) $5d_{yz}\rightarrow\pi^*_{bpy}$ (33%)	**32830** (29870)	**305**	**0.140**	**25840**	**387**
c^1MLCT c^1A'	$5d_{yz}\rightarrow\pi^*_{bpy}$ (59%) $5d_{x^2-y^2}\rightarrow\pi^*_{bpy}$ (34%)	**33700** (31650)	**297**	**0.209**	**26800**	**373**
^{3}LLCT b^3A''	$\pi_{stpy}\rightarrow\pi^*_{bpy}$ (88%)	36 670			28190	
^{1}LLCT b^1A''	$\pi_{stpy}\rightarrow\pi^*_{bpy}$ (89%)	36810	272	0.003	28400	
^{1}IL d^1A'	$\pi_{stpy}\rightarrow\pi^*_{stpy}$ (91%)	**37950** (38350)	**264**	**1.512**	**23130**	

[a] In parenthesis CASSCF transition energies of the conformer A of C_1 symmetry for which the PEC have been computed.

The perturbational treatment has some difficulties in correctly describing the corresponding ^{1}IL. This failure is due to the limitation of the CASSCF active space, which should include the totality of the π system of the stpy ligand (fourteen electrons π-correlated in fourteen bonding and antibonding orbitals). This feature has been well documented by previous theoretical studies on stilbene-like molecules.[27,32] A huge active space would be needed to describe this part of the electronic correlation at the zero-order in the CASSCF wavefunction.

Potential energy curves describing the *trans*-[Re(stpy)(CO)$_3$(bpy)]$^+$ to *cis*-[Re(stpy)(CO)$_3$(bpy)]$^+$ isomerization, a CASSCF analysis: According to the previous sections, the electronic absorption spectrum of [Re(stpy)(CO)$_3$(bpy)]$^+$ is qualitatively well described at the CASSCF level with a systematic overestimation of the transition energies by about 1.0 eV (8000 cm^{-1}). To follow the evolution of the ^{1}MLCT and ^{1}IL absorbing states and of the corresponding ^{3}IL and ^{3}MLCT states as a function of the angular torsion of the C=C bond (θ) in the stpy ligand, PECs have been computed at the CASSCF level (eight electrons correlated in nine orbitals, state average over five to six roots). Other secondary modes such as the rotation of the benzenic and pyridinic rings, the elongation of the double bond, or the carbon pyramidalization are neglected in this qualitative study, which focuses on the electronic dimensionality. Moreover this approximation is justified by the presence of a heavy atom, which may reduce the nuclear flexibility of the molecule relative to the organic free ligands such as stilbene or azobenzene. The initial geometry (θ = 0°) corresponds to the structure of the *trans*-[Re(stpy)(CO)$_3$(bpy)]$^+$ conformer A (Figure 3), and the C_1 symmetry has been retained along the reaction pathway. The corresponding CASSCF transition energies are reported in Table 3. They do not differ drastically from the transition energies obtained for the conformer B with two nearly degenerate ^{1}MLCT absorbing states at about 29860 and 29870 cm^{-1}, one strongly absorbing MLCT state at 31650 cm^{-1}, and the ^{1}IL state calculated at 38350 cm^{-1}. The corresponding triplet states are at 24530 cm^{-1} (^{3}IL), and range between 25280 and 28060 cm^{-1} (^{3}MLCT). The calculated PEC corresponding to the electronic ground state ^{1}A, the three low-lying a^{1}MLCT, b^{1}MLCT, and c^{1}MLCT states, the ^{1}IL state, the three low-lying ^{3}MLCT states, and the ^{3}IL state, for values of θ varying between 0° and 90°, are depicted in Figure 6. The corresponding energy values are reported in Table 4.

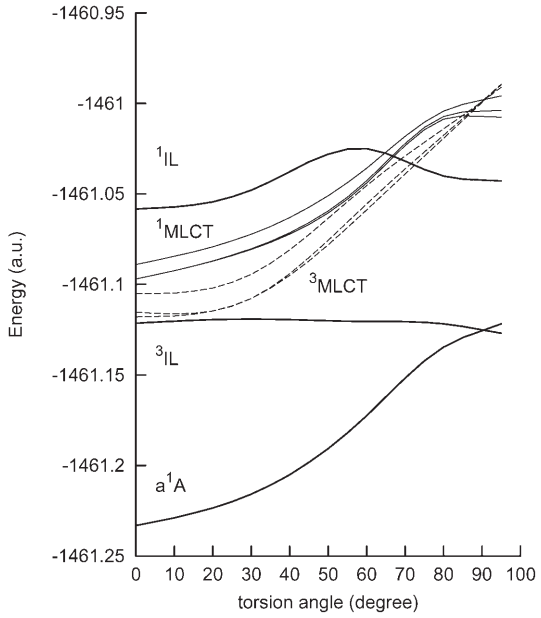

Figure 6. CASSCF PECs corresponding to the low-lying singlet and triplet (dashed lines) excited states of [Re(CO)$_3$(bpy)(stpy)]$^+$ as a function of the torsion angle θ of the carbon–carbon double bond of the styrylpyridine ligand.

Table 4. CASSCF energies [a.u. −1461] of the electronic ground state a^{1}A, the low-lying ^{1,3}MLCT states, and ^{1,3}IL states of [Re(CO)$_3$(bpy)(stpy)]$^+$ as a function of θ. The values in italic correspond to the CASSCF calculations limited to three electronic states, namely the a^{1}A ground state and the ^{1,3}IL states (the weights on the a^{1}A electronic ground state and on the ^{1}IL state are given in parenthesis).

State θ	0°	30°	60°	80°	90°	100°	120°
a^{1}A	**0.23312**	**0.21576**	**0.17244**	**0.13447**	**0.12553**		
		0.23480	*0.18888*	*0.14854*	*0.13664*	*0.14355*	*0.17296*
		(93%)	*(59%)*	*(23%)*	*(<5%)*	*(20%)*	*(59%)*
^{3}IL	**0.12133**	**0.11906**	**0.12035**	**0.12170**	**0.12500**		
	0.15876	*0.16080*	*0.16171*	*0.15954*	*0.15812*	*0.15643*	–
a^{3}MLCT	0.11792	0.10779	0.05885	0.01929	–		
b^{3}MLCT	0.11537	0.10465	0.05553	0.01752	–		
c^{3}MLCT	0.10526	0.09452	0.04543	0.01400	–		
a^{1}MLCT	0.09707	0.08065	0.04391	0.00869	0.00726		
b^{1}MLCT	0.09704	0.08028	0.04271	0.00723	0.00349		
c^{1}MLCT	0.08893	0.07223	0.03574	0.00422	0.00178		
^{1}IL	**0.05837**	**0.04796**	**0.02502**	**0.04017**	**0.04235**		
		0.07930	*0.07575*	*0.09532*	*0.10204*	*0.09350*	*0.06616*
		(93%)	*(59%)*	*(23%)*	*(<5%)*	*20%*	*(59%)*

The energy of the a^{1}A electronic ground state increases as a function of the torsion angle to reach a maximum at the perpendicular geometry (θ = 90°). At the same time the weight varies from 91% for the $(\pi_{C=C})^2(5d_{yz})^2(5d_{xz})^2(5d_{xy})^2(\pi^*_{C=C})^0$ electronic configuration at the equilibrium geometry, to 90% for the $(\pi_{C=C})^1(5d_{yz})^2(5d_{xz})^2(5d_{xy})^2(\pi^*_{C=C})^1$ electronic configuration at the perpendicular geometry, in which the π bonding does not exist anymore. The $\pi_{C=C}$ orbital is purely localized on one carbon atom of the C=C bond of the styrylpyridine and the $\pi^*_{C=C}$ orbital on the other one.

At this point, corresponding to the diradical formation at the level of the C=C bond, the ^{3}IL state characterized by a nearly flat PEC is quasi-degenerate with the a^{1}A state. The

energy profile of the corresponding ^{1}IL state affords an energy barrier of about 0.62 eV at $\theta = 60°$ and an energy gap of 2.19 eV with the a^{1}A state at $\theta = 90°$. At the equilibrium geometry the ^{1}IL is characterized by a weight of 91% for the $(\pi_{C=C})^1(5d_{yz})^2(5d_{xz})^2(5d_{xy})^2(\pi^*_{C=C})^1$ electronic configuration. This weight decreases to 66% (at the barrier), at which point the state gains some character from the double excited state corresponding to the $(\pi_{C=C})^0$ $(5d_{yz})^2(5d_{xz})^2$-$(5d_{xy})^2(\pi^*_{C=C})^2$ configuration. The interaction between these two states generates an avoided crossing responsible for the observed energy barrier. At $\theta = 90°$ the ^{1}IL state becomes nearly pure with 91% for the $(\pi_{C=C})^2(5d_{yz})^2(5d_{xz})^2(5d_{xy})^2$-$(\pi^*_{C=C})^0$ electronic configuration in which $\pi_{C=C}$ is purely localized on one carbon atom of the C=C bond of the styrylpyridine and $\pi^*_{C=C}$ on the other one. The three low-lying ^{1}MLCT states as well as the corresponding ^{3}MLCT states are strongly bound with respect to the angular torsion of the C=C bond of the styrylpyridine ligand within the limit of the one-dimensional model. For the sake of clarity allowed crossings are represented between the ^{1}IL state and the MLCT states. If this picture is correct for the ^{3}MLCT states, avoided crossings should occur between the ^{1}MLCT and ^{1}IL adiabatic PEC. However this simplified representation should not modify our analysis of the mechanism of *trans–cis* photoisomerization represented in Figure 7.

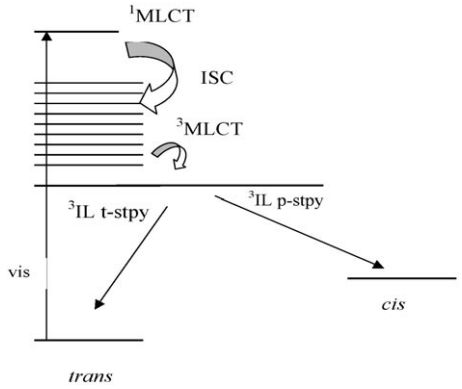

Figure 7. Simplified representation of the mechanism of the *trans–cis* photoisomerization.

After excitation to the c^{1}MLCT state corresponding to a $d_{Re}\rightarrow\pi^*_{bpy}$ excitation, the system could populate the lowest ^{1}MLCT and ^{3}MLCT state by means of internal conversion and intersystem crossing, respectively. During these elementary processes, which should occur within the picosecond (ps) time scale, there is no deactivation channel towards the perpendicular intermediate, owing to the bound character of the MLCT states. The role of the rhenium center is to switch the mechanism from the ^{1}IL state in the free organic ligands (stilbene, azobenzene) to the ^{3}IL state by a fast ^{3}MLCT$\rightarrow^3$IL internal conversion (~3.5 ps according to the experiments).[6] From this state the system may progress along the ^{3}IL PEC towards the perpendicular intermediate in the ^{3}IL$_p$ state degenerate with the a^{1}A state and evolve either back to the *trans*-[Re(stpy)(CO)$_3$(bpy)]$^+$ complex or to the *cis*-[Re(stpy)(CO)$_3$(bpy)]$^+$ isomer. The flat shape of the ^{3}IL PEC may explain the rather slow, experimentally determined rotation of 90° around the C=C bond of the styrylpyridine (~12 ps).[6] The coordination to the metal center acts as a triplet photosensitization and the rate-determining step to reach the ^{3}IL is the ^{1}MLCT$\rightarrow^3$MLCT intersystem crossing. The presence of the low-lying MLCT states enables the photoisomerization process to occur after visible irradiation instead of UV irradiation in the free organic compounds. The isomerization quantum yield of [Re(stpy)(CO)$_3$(bpy)]$^+$ was reported to be very low.[5] According to the mechanism depicted in Figure 7 this could be due to the presence of concurrent deactivation channels from the low-lying MLCT states to the electronic ground states. However there is no experimental evidence of such luminescent processes.[6] Another aspect concerns vibrational relaxation effects in the low-lying MLCT states, which may be active for the isomerization process. Indeed other nuclear deformations that are not taken into account in this simplified one-dimensional model may support the isomerization process.

To compare the mechanism of photoisomerization of [Re(stpy)(CO)$_3$(bpy)]$^+$ with that of free organic ligands,[7–9,33–35] PECs corresponding to the a^{1}A ground state and to the ^{1,3}IL state of [Re(stpy)(CO)$_3$(bpy)]$^+$ have been computed by means of state-specific CASSCF (^{3}IL) and of two states average CASSCF (a^{1}A, ^{1}IL) with the same active space characteristics but without the low-lying MLCT states. These PECs calculated as a function of θ between 0° (*trans* isomer) and 120° are represented in Figure 8 and the corresponding energies values are reported in Table 4. The a^{1}A

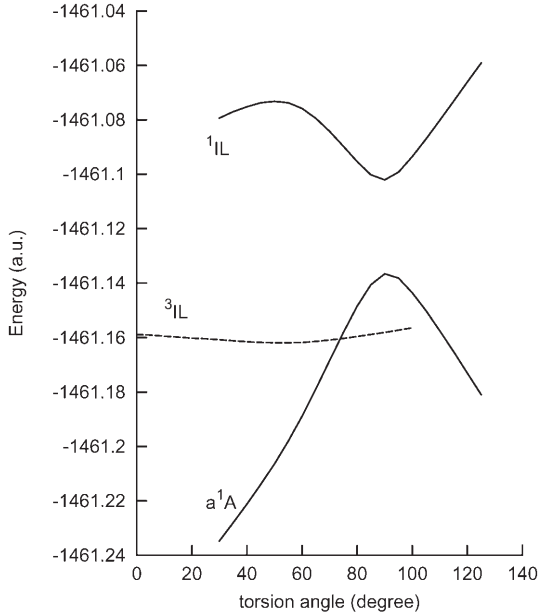

Figure 8. CASSCF PECs corresponding to the electronic ground state and the ^{1,3}IL excited states of [Re(CO)$_3$(bpy)(stpy)]$^+$ as a function of the torsion angle θ of the carbon–carbon double bond of the styrylpyridine ligand.

electronic ground state, called the S_0 state in the stilbene-like molecules, presents an energy barrier with a maximum at the perpendicular geometry corresponding to an angle of 90° and to a diradical with the electronic configurations described above. The ^{3}IL PEC is nearly flat with a crossing with the a^1A ground state PEC before 80° earlier than the one observed in Figure 6 on the whole set of PECs. The ^{1}IL PEC corresponding to the S_1 state in the free organic ligand presents an energy barrier before 60° and an avoided crossing with the electronic ground state PEC. A careful analysis of the CASSCF weights (see Table 4) points to a clear change of electronic configuration between 60° and 120° with a completely symmetric exchange between the a^1A and ^{1}IL states. The ^{3}IL state remains nearly pure along the photoisomerization pathway with a weight of 93%.

According to this qualitative picture the position of the crossing point between the ^{3}IL and the electronic ground state PEC could control the quantum yield of the photoisomerization process leading to an asymmetric mechanism. In the less favorable case such as the one depicted in Figure 8 this crossing occurs too early along the torsion coordinate to reach the maximum of the energy barrier and to lead to the *cis* isomer. Again the limitation of the one-dimensional model restricted to the torsion angle around the C=C bond of the styrylpyridine ligand does not allow any conclusions, but according to experimental data steric constraints in the low-symmetry $[Re(stpy)(CO)_3(bpy)]^+$ complex investigated in the present work could be responsible for such inefficient photoisomerizations.

Conclusion

On the basis of a careful theoretical analysis of the structures, electronic spectroscopy, and evolution of the potential energy of the low-lying IL and MLCT excited states of $[Re(CO)_3(bpy)(stpy)]^+$ as a function of the carbon–carbon double bond torsion angle of the styrylpyridine, it has been shown that the photoisomerization of the ligand under visible light operates by a triplet intraligand mechanism via the ^{3}IL ($\pi_{stpy}\rightarrow\pi^*_{stpy}$) state. This state is populated by intramolecular energy transfer from the $Re^I(CO)_3(bpy)$ chromophore to the styrylpyridine ligand. The early photoisomerization dynamics (within a few ps) is governed by the evolution of the system from the ^{1}MLCT absorbing state to the ^{3}IL via the set of low-lying ^{3}MLCT states in the Franck–Condon region. The *trans–cis* isomerization of the styrylpyridine ligand is preceded by a rotation of about 90° around the carbon–carbon double bond in the ^{3}IL state. At about the perpendicular conformation the ^{3}IL state potential crosses the ground state potential. The isomerization process occurs after intersystem crossing on the electronic ground state potential energy surface from the perpendicular conformation of the ligand, according to the mechanism proposed for the free ligand. The role of the rhenium is to switch the mechanism from the ^{1}IL state accessible through UV irradiation in the free organic ligand to the ^{3}IL state easily reached after visible excitation to the low-lying MLCT states. The metal-to-styrylpyridine charge-transfer states do not participate in the mechanism of photoisomerization. The calculated theoretical picture of the photochemical mechanism agrees remarkably well with the experimental mechanism proposed by Busby et al.[6]

Acknowledgements

This work was undertaken as a part of the European collaborative COST projects (D14/0001/99 and COST D35). The calculations were carried out in part at the Centre Universitaire et Régional de Ressources Informatiques (CURRI, Université Louis Pasteur, Strasbourg), in part at the IDRIS and CINES computer centers (CNRS, Orsay, Montpellier) through a grant of computer time from the Conseil Scientifique and at the LCQS (Strasbourg).

[1] D. J. Stufkens, A. Vlček Jr., *Coord. Chem. Rev.* **1998**, *177*, 127; I. R. Farrell, P. Matousek, C. J. Kleverlaan, A. Vlček Jr., *Chem. Eur. J.* **2000**, *6*, 1386.
[2] D. Brent MacQueen, K. S. Schanze, *J. Am. Chem. Soc.* **1991**, *113*, 6108; J. D. Lewis, L. Bussotti, P. Foggi, R. N. Perutz, J. N. Moore, *J. Phys. Chem. A* **2002**, *106*, 12202.
[3] K. Kalyanasundaram, *Photochemistry of Polypyridine and Porphyrin Complexes*, Academic Press, London, **1992**; O. Horváth, K. L. Stevenson, *Charge Transfer Photochemistry of Coordination Compounds*, VCH, New York, **1993**; *Energy Resources through Photochemistry and Catalysis* (Ed.: M. Gratzel), Academic Press, New York, **1983**.
[4] V. Balzani, F. Scandola, *Supramolecular Photochemistry*, Ellis Horwood, Chichester, **1991**.
[5] V. W. W. Yam, V. C. Y. Lau, K. K. Cheung, *J. Chem. Soc. Chem. Commun.* **1995**, 259; V. W. W. Yam, V. C. Y. Lau, K. K. Cheung, *J. Chem. Soc. Chem. Commun.* **1995**, 1195; V. W. W. Yam, V. C. Y. Lau, L. X. Wu, *J. Chem. Soc. Dalton Trans.* **1998**, 1461.
[6] M. Busby, P. Matousek, M. Towrie, A. Vlček Jr., *J. Phys. Chem. A* **2005**, *109*, 3000.
[7] G. Orlandi, P. Palmieri, G. Poggi, *J. Am. Chem. Soc.* **1979**, *101*, 3492; D. H. Waldeck, *Chem. Rev.* **1991**, *91*, 415.
[8] J. A. Syage, P. M. Felker, A. H. Zewail, *J. Chem. Phys.* **1984**, *81*, 4706; P. Gajdek, R. S. Becker, F. Elisei, U. Mazzucato, A. Spalletti, *J. of Photochem. Photobiol. A: Chem.* **1996**, *100*, 57; A. A. Heikal, J. S. Baskin, L. Baòares, A. H. Zewail, *J. Phys. Chem. A* **1997**, *101*, 572.
[9] J. Quenneville, T. J. Martinez, *J. Phys. Chem. A* **2003**, *107*, 829.
[10] C. Lee, W. Yang, R. G. Parr, *Phys. Rev. B* **1988**, *37*, 785.
[11] A. D. Becke, *J. Chem. Phys.* **1993**, *98*, 5648.
[12] B. O. Roos, *Int. J. Quantum Chem.* **1980**, *14*, 175; B. O. Roos, P. Taylor, P. E. M. Siegbahn, *Chem. Phys.* **1980**, *48*, 157.
[13] K. Andersson, P. Å. Malmqvist, B. O. Roos, A. J. Sadlej, . K. J. Wolinski, *Phys. Chem.* **1990**, *94*, 5483; K. Andersson, P.-Å. Malmqvist, B. O. Roos, *J. Chem. Phys.* **1992**, *96*, 1218.
[14] C. Jamorski, M. E. Casida, D. R. Salahub, *J. Chem. Phys.* **1996**, *104*, 5134.
[15] B. O. Roos, K. Andersson, *Chem. Phys. Lett.* **1995**, *245*, 215.
[16] J. Bossert, PhD Thesis, Université Louis Pasteur, Strasbourg (France), **2004**.
[17] D. Andrae, U. Haeussermann, M. Dolg, H. Stoll, H. Preuss, *Theor. Chim. Acta* **1990**, *77*, 123; A. Bergner, M. Dolg, W. Küchle, H. Stoll, H. Preuss, *Mol. Phys.* **1993**, *80*, 1431.
[18] J. T. H. Dunning, P. J. Hay in *Methods for Electronic Structure Theory* (Ed.: H. F. Schaefer III), Plenum, New York, **1977**, pp. 1–28.
[19] K. Pierloot, B. Dumez, P.-O. Widmark, B. O. Roos, *Theor. Chim. Acta* **1995**, *90*, 87.
[20] J. T. H. Dunning, *J. Chem. Phys.* **1989**, *90*, 1007.

[21] M. J. Frisch, G. W. Trucks, H. B. Schlegel, G. E. Scuseria, M. A. Robb, J. R. Cheesemann, V. G. Zakrzewski, J. A. Montgomery Jr., R. E. Stratmann, J. C. Burant, S. Dapprich, J. M. Millam, A. D. Daniels, K. N. Kudin, M. C. Strain, O. Farkas, J. Tomasi, V. Barone, M. Cossi, R. Cammi, B. Mennuci, C. Pomelli, C. Adamo, S. Clifford, J. Ochterski, G. A. Petersson, P. Y. Ayala, Q. Cui, K. Morokuma, D. K. Malick, A. D. Rabuck, K. Raghavachari, J. B. Foresman, J. Cioslowski, J. V. Ortiz, B. B. Stefanov, G. Liu, A. Liashenko, P. Piskorz, I. Komaromi, R. Gomperts, R. L. Martin, D. J. Fox, T. Keith, M. A. Al-Laham, C. Y. Peng, A. Nanayakkara, C. Gonzalez, M. Challacombe, P. M. W. Gill, B. Johnson, W. Chen, M. W. Wong, J. L. Andres, C. Gonzalez, M. Head-Gordon, E. S. Replogle, J. A. Pople, Gaussian 98, Gaussian, Inc, Pittsburgh, PA (USA) **1998**.

[22] K. Andersson, M. Barysz, A. Bernhardsson, M. R. A. Blomberg, D. L. Cooper, M. P. Fülscher, C. de Graaf, B. A. Hess, G. Karlström, R. Lindh, P.-Å. Malmqvist, T. Nakajima, P. Neogrády, J. Olsen, B. O. Roos, B. Schimmelpfennig, M. Schütz, L. Seijo, L. Serrano-Andrés, P. E. M. Siegbahn, J. Stålring, T. Thorsteinsson, V. Veryazov, P.-O. Widmark, Molcas, Version 5.4, Lund University, Sweden **2002**.

[23] M. Busby, D. J. Liard, M. Motevalli, H. Toms, A. Vlèek Jr, *Inorg. Chim. Acta* **2004**, *357*, 167.

[24] V. W. W. Yam, Y. Yang, J. Zhang, B. W. K. Chu, N. Zhu, *Organometallics* **2001**, *20*, 4911.

[25] V. M. Chapela M. J. Percino, Rodriguez-Barbarin, *J. Chem. Crystallogr.* **2003**, *33*, 77.

[26] K. Ogawa, J. Harada, S. Tomoda, *Acta Crystallogr. Sect. B* **1995**, *51*, 240.

[27] V. Molina, M. Merchán, B. O. Roos, *J. Phys. Chem. A* **1997**, *101*, 3478; V. Molina, M. Merchán, B. O. Roos, *Spectrochim. Acta Part A* **1999**, 55, 433.

[28] A. Vlèek Jr., private communication.

[29] A. Dreuw, M. Head-Gordon, *J. Am. Chem. Soc.* **2004**, *126*, 4007.

[30] A Dreuw, J. L. Weisman, M. Head-Gordon, *J. Chem. Phys.* **2003**, *119*, 2943.

[31] O. Gritsenko , E. J. Baerends, *J. Chem. Phys.* **2004**, *121*, 655.

[32] L. Gagliardi, G. Orlandi, V. Molina, P.-Å Malmqvist, B. O. Roos, *J. Phys. Chem. A* **2002**, *106*, 7355.

[33] L. Gagliardi, G. Orlandi, F. Bernardi, A. Cembran, M. Garavelli, *Theor. Chem. Acc.* **2004**, *111*, 363; A. Cembran, F. Bernardi, M. Garavelli, L. Gagliardi, G. Orlandi, *J. Am. Chem. Soc.* **2004**, *126*, 3234.

[34] T. Schultz, J. Quenneville, B. Levine, A. Toniolo, T. J. Martinez, S. Lochbrunner, M. Schmitt, J. P. Shaffer, M. Z. Zgierski, A. Stolow, *J. Am. Chem. Soc.* **2003**, *125*, 8098.

[35] C. Ciminelli, G. Granucci, M. Persico, *Chem. Eur. J.* **2004**, *10*, 2327.

Received: September 2, 2005
Revised: October 10, 2005
Published online: April 27, 2006

